Electronic Supplementary Material (ESI) for Physical Chemistry Chemical Physics


# Photothermal Signal Distribution Analysis (PhoSDA): Supplement

Markus Selmke, Marco Braun, Romy Schachoff and Frank Cichos

January 7, 2013

## 1 Histograms

We will consider the following azimuthally symmetric signal function $\Phi(\mathbf{r})$ which we found to approximate the true PT detection volume well[1]. We will use cylindrical coordinates $\mathbf{r} = (\rho\cos\phi, \rho\sin\phi, z)$.

$$\Phi(z,\rho) = \Phi_0 \exp\left(-\frac{2\rho^2}{\omega_\rho^2}\right)[z_0 - z]\exp\left(-\frac{2z^2}{\omega_z^2}\right) \tag{1}$$

The amplitude $\Phi_0$, which has the units of an inverse length unit, quantifies the rel. PT signal of the particle. Thus, for small particles it scales with the volume, i.e. $\Phi_0 \propto R^3$. The maximum signal $\Phi_{\text{max}}$ is obtained at $z_+ = [z_0 - \delta_{\text{pp}}]/2$ while the minimum signal $\Phi_{\text{min}}$ is obtained at $z_- = [z_0 + \delta_{\text{pp}}]/2$ with the positive axial peak-to-peak distance $\delta_{\text{pp}}$ of the detection volume eqn (1) given as $\delta_{\text{pp}}^2 = z_0^2 + \gamma^2\omega_\rho^2$. The maximum signal is $\Phi_{\text{max}} = \Phi(z_+)$ while the minimum signal is $\Phi_{\text{min}} = \Phi(z_-)$. Equation 1 may be inverted to yield the radius $\rho$ as a function of $z$ for a given signal value $\Phi$:

$$\rho(z,\Phi) = \frac{\omega_\rho}{\sqrt{2}}\left[-\frac{2z^2}{\omega_z^2} + \log\left(\frac{[z_0 - z]\Phi_0}{\Phi}\right)\right]^{1/2} \tag{2}$$

In the previous expression, $\Phi$ was used to denote a specific signal value, i.e. the equation $\Phi(z,\rho) = \Phi$ was solved for $\rho$. From this equation one may readily show that the following relation holds:

$$\rho(z,\Phi)\frac{\mathrm{d}\rho(z,\Phi)}{\mathrm{d}\Phi} = -\frac{\omega_\rho^2}{4\Phi} \tag{3}$$

Now, $z_1$ and $z_2$ will denote the two roots of the transcendental equation $\Phi_0[z_0 - z]\exp\left(-\frac{2z^2}{\omega_z^2}\right) = \Phi$, i.e. the axial coordinate at which the *signal value* $\Phi$ is attained by the *function* $\Phi(z,0)$. The occurrence of a certain signal value $\Phi$ within an interval $I_\Phi = [\Phi, \Phi + \Delta\Phi]$ will be proportional to the volume $V$ which covers the space in which the signal function $\Phi(z,\rho)$ is within this range for some small but fixed $\Delta\Phi$. The following approximation to first order in the small quantity $\Delta\Phi$ will be used in the derivation which follows:

$$[\rho(z,\Phi+\Delta\Phi)]^2 \approx \left[\rho(z,\Phi) + \frac{\mathrm{d}\rho(z,\Phi)}{\mathrm{d}\Phi}\Delta\Phi\right]^2 \approx \rho(z,\Phi)^2 + 2\rho(z,\Phi)\frac{\mathrm{d}\rho(z,\Phi)}{\mathrm{d}\Phi}\Delta\Phi + \mathcal{O}\left(\Delta\Phi^2\right) \tag{4}$$

Electronic Supplementary Material (ESI) for Physical Chemistry Chemical Physics




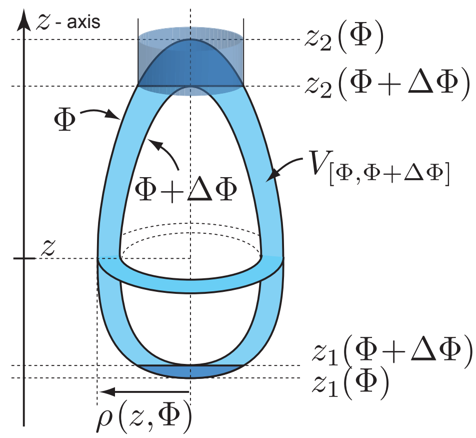


Figure 1: Sketch for the volume integration. $\Delta\Phi > 0$.

We obtain for the volume belonging to the signal range $[\Phi, \Phi + \Delta\Phi]$:

$$\begin{aligned} V_{[\Phi,\Phi+\Delta\Phi]} &= 2\pi\left[\int_{z_1(\Phi)}^{z_2(\Phi)}\int_0^{\rho(z,\Phi)}\rho\mathrm{d}\rho\mathrm{d}z - \int_{z_1(\Phi+\Delta\Phi)}^{z_2(\Phi+\Delta\Phi)}\int_0^{\rho(z,\Phi+\Delta\Phi)}\rho\mathrm{d}\rho\mathrm{d}z\right] \\ &= 2\pi\left[\int_{z_1(\Phi)}^{z_2(\Phi)}\frac{\rho\left(z,\Phi\right)^2}{2}\mathrm{d}z - \int_{z_1(\Phi+\Delta\Phi)}^{z_2(\Phi+\Delta\Phi)}\frac{\rho\left(z,\Phi+\Delta\Phi\right)^2}{2}\mathrm{d}z\right] \\ &= 2\pi\left[\int_{z_1(\Phi+\Delta\Phi)}^{z_2(\Phi+\Delta\Phi)}\left(\frac{\rho\left(z,\Phi\right)^2}{2} - \frac{\rho\left(z,\Phi+\Delta\Phi\right)^2}{2}\right)\mathrm{d}z\right] + V_2 \\ &\approx -2\pi\Delta\Phi\int_{z_1(\Phi+\Delta\Phi)}^{z_2(\Phi+\Delta\Phi)}\left(\rho\left(z,\Phi\right)\frac{\mathrm{d}\rho\left(z,\Phi\right)}{\mathrm{d}\Phi}\right)\mathrm{d}z \quad\approx\quad \frac{\Delta\Phi}{\Phi}\frac{\pi\omega_\rho^2}{2}\left[z_2\left(\Phi,\Phi_0\right) - z_1\left(\Phi,\Phi_0\right)\right] \end{aligned} \tag{5}$$

where the small cap-volumes $V_2$ have been neglected since they are of order $\mathcal{O}\left(\Delta\Phi^2\right)$ as may be seen from an upper pill-box estimate of the volume $V_2$ (see Fig. 1):

$$\begin{aligned} V_2 &= 2\pi\left[\int_{z_1(\Phi)}^{z_1(\Phi+\Delta\Phi)}\frac{\rho^2\left(z,\Phi\right)}{2}\mathrm{d}z + \int_{z_2(\Phi+\Delta\Phi)}^{z_2(\Phi)}\frac{\rho^2\left(z,\Phi\right)}{2}\mathrm{d}z\right] \\ &< \pi\left[z_1\left(\Phi+\Delta\Phi\right) - z_1\left(\Phi\right)\right]\rho^2\left(\Phi, z_1\left(\Phi+\Delta\Phi\right)\right) \quad + \quad \pi\left[z_2\left(\Phi\right) - z_2\left(\Phi+\Delta\Phi\right)\right]\rho^2\left(\Phi, z_2\left(\Phi+\Delta\Phi\right)\right) \\ &= \pi\left(\frac{\partial z_1\left(\Phi\right)}{\partial\Phi}\Delta\Phi\right)\left[\rho^2\left(\Phi,z_1\right) + \frac{\partial\rho^2}{\partial z}\frac{\partial z_1\left(\Phi\right)}{\partial\Phi}\Delta\Phi\right] + \pi\left(-\frac{\partial z_2\left(\Phi\right)}{\partial\Phi}\Delta\Phi\right)\left[\rho^2\left(\Phi,z_2\right) + \frac{\partial\rho^2}{\partial z}\frac{\partial z_2\left(\Phi\right)}{\partial\Phi}\Delta\Phi\right] \\ &= \pi\Delta\Phi^2 \times \left[\left(\frac{\partial z_1\left(\Phi\right)}{\partial\Phi}\right)^2\frac{\partial\rho^2}{\partial z} - \left(\frac{\partial z_2\left(\Phi\right)}{\partial\Phi}\right)^2\frac{\partial\rho^2}{\partial z}\right] \end{aligned} \tag{6}$$

where $\rho^2\left(\Phi,z_2\right) = \rho^2\left(\Phi,z_1\right) = 0$ was used in the last step. The smallness of $V_2$ relative to $V_{[\Phi,\Phi+\Delta\Phi]}$ as approximated above was also checked numerically. For a wide range of typical parameters and

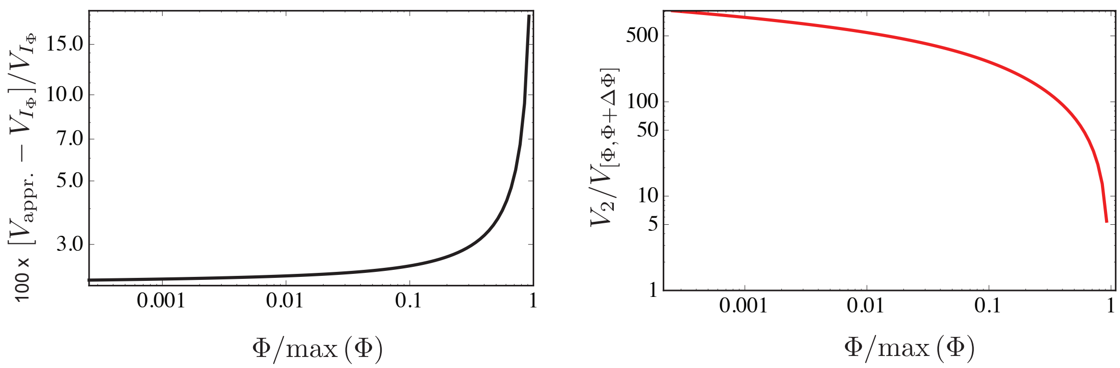


Figure 2: (Left) Relative difference in percent between the approximation eqn (5) and the result of a numerical integration for the exact value of $V_{I_\Phi}$ normalized to the exact value. (Right) Relative fraction of the cap-volumes $V_2$ by the total volume $V_{I_\Phi}$.

typical number of about 100 logarithmically spaced bins of width $[\Phi_{i+1} - \Phi_i]/2$ one find that the relative error is less then 15 percent, see Fig. 2. Also, one can see that indeed the fraction of the volume associated with $V_2$ is small compared to the total volume $V_{I_\Phi}$.

This finally gives the expression stated in the main article which is strictly true only for an infinitesimal bin width $\mathrm{d}\Phi$:

$$p(\Phi, \Phi_0)\,\mathrm{d}\Phi \propto \frac{\pi\omega_\rho^2}{2\Phi}\left[z_2(\Phi, \Phi_0) - z_1(\Phi, \Phi_0)\right]\mathrm{d}\Phi \tag{7}$$

## 1.1 Details on histograms with size dispersion

For the description of the histograms of particles with size dispersion we will assume $\Phi \propto R^3$ which is true for small particles in the Rayleigh regime. Therefore, with the normalization to the largest particles appearing $\Phi_0(R) = R^3/R_{\text{max}}^3$ (whereby we set the amplitude of the largest particles signal shape to one, $\Phi_0(R_{\text{max}}) = 1$), we may rewrite the expression for the mono-disperse histogram to $p(\Phi, \Phi_0)|_R = p(\Phi/\Phi_0, \Phi_0 = 1)/\Phi_0$ with $\Phi \in [\Phi_{\text{min}}|_{\Phi_0=1}, \Phi_{\text{max}}|_{\Phi_0=1}]$ via substitution of variables. Hence, by assuming a size dispersion described by $p_R(R) = \exp(-[R - \langle R\rangle]^2/[2\sigma_R^2])$ and $R \in [R_{\text{min}}, R_{\text{max}}]$, we get the histogram from the following equation.

$$\begin{aligned} p\left(\frac{\Phi}{\Phi_{\text{max}}(R_{\text{max}})}, \langle R\rangle, \sigma_R\right) &= \frac{\int_{R_{\text{min}}}^{R_{\text{max}}} p\left(\Phi, \frac{R^3}{R_{\text{max}}^3}\right)\Big|_R \times p_R(R)\,\mathrm{d}R}{\int_{R_{\text{min}}}^{R_{\text{max}}} p_R(R)\,\mathrm{d}R} \\ &= \frac{\int_{R_{\text{min}}}^{R_{\text{max}}} p\left(\Phi\frac{R_{\text{max}}^3}{R^3}, 1\right) \times \frac{R_{\text{max}}^3}{R^3} \times p_R(R)\,\mathrm{d}R}{\int_{R_{\text{min}}}^{R_{\text{max}}} p_R(R)\,\mathrm{d}R} \end{aligned} \tag{8}$$

Note, that there is a critical minimum radius $R_c(\Phi)$ of particles contributing to the signal occurrence of the signal value $\Phi$, i.e. the probability density is zero $p\left(\Phi \times R_{\text{max}}^3/R^3, 1\right) = 0$ for particles smaller than $R < R_c(\Phi)$. Equivalently, the signal value $\Phi \notin \left[\Phi_{\text{min}}|_{\Phi_0(R)}, \Phi_{\text{max}}|_{\Phi_0(R)}\right]$ for $R < R_c$ (see Fig. 3).

Electronic Supplementary Material (ESI) for Physical Chemistry Chemical Physics




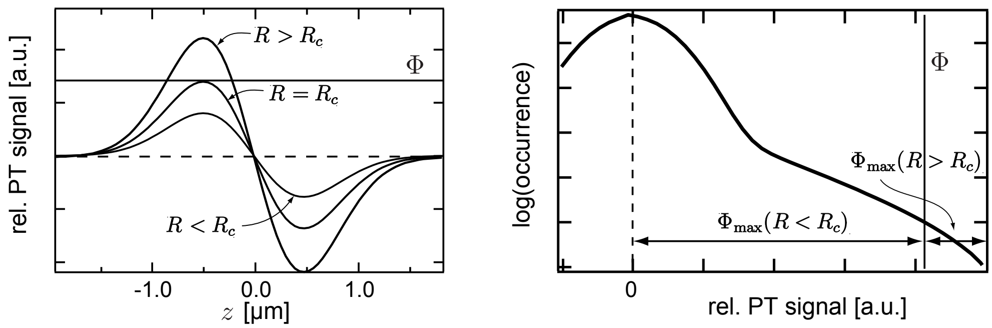


Figure 3: Sketch of the PT signal along the optical axis for three different particle sizes, but the same heating intensity: only particles of radius $R \geq R_c$ larger than the critical radius $R_c$ can contribute in the histogram at a certain PT signal strength $\Phi$. Particles of smaller size can not reach a PT signal strength $\Phi$ within the focal detection volume. Hence, the sharp cutoff in the histograms obtained for mono-disperse particles at $\Phi_{\max}$ is blurred in the case of particles with a size dispersion (see also Fig. 5 in the main article).

## 1.2 Histograms: simple 3D-Gaussian

Now the special case of a 3D-Gaussian detection volume is assumed. This functional form approximates well the case of a maximal PT signal configuration with an axial laser-offset of about $\Delta z_f \approx \pm z_R$ [1,2].

$$\Phi\left(z,\rho\right) = \Phi_0 \exp\left(-\frac{2\rho^2}{\omega_\rho^2}\right)\exp\left(-\frac{2z^2}{\omega_z^2}\right) \tag{9}$$

The equation may be inverted to yield the radius $\rho$ as a function of $z$ for a given signal $\Phi$:

$$\rho\left(z,\Phi\right) = \left[\frac{\omega_\rho^2}{2}\log\left(\frac{\exp\left(-\frac{2z^2}{\omega_z^2}\right)\Phi_0}{\Phi}\right)\right]^{1/2} = \frac{\omega_\rho}{\sqrt{2}}\left[-\frac{2z^2}{\omega_z^2} - \log\left(\frac{\Phi}{\Phi_0}\right)\right]^{1/2} \tag{10}$$

inverting the on-axis signal expression $\Phi_0 \exp\left(-2z^2/\omega_z^2\right) = \Phi$ yields the maximum z-values for a specific signal $\Phi$: $z_{1,2} = \pm\left[\ln\left(\Phi/\Phi_0\right)\omega_z^2/\left(-2\right)\right]^{1/2}$. Also, $\rho \mathrm{d}\rho/\mathrm{d}\Phi = -\omega_\rho^2/\left(4\Phi\right)$, and thus we obtain:

$$V_{[\Phi,\Phi+\Delta\Phi]} = \Delta\Phi\frac{\pi\omega_\rho^2}{2\Phi}\left[z_1\left(\Phi\right) - z_2\left(\Phi\right)\right] = \frac{\Delta\Phi}{\Phi}\frac{\pi\omega_\rho^2}{2}2\left[\frac{\omega_z^2\ln\left(\Phi/\Phi_0\right)}{-2}\right]^{1/2} = \frac{\Delta\Phi}{\Phi}\frac{\pi\,\gamma\omega_\rho^3}{\sqrt{2}}\sqrt{\ln\left(\frac{\Phi_0}{\Phi}\right)} \tag{11}$$

Now, using $V_{\text{eff}} = \pi^{3/2}\gamma\omega_\rho^3$as detailed in the supplement of Ref. [1], one finds the expression stated in the main article:

$$p\left(\Phi,\Phi_0\right)\mathrm{d}\Phi \propto \frac{V_{\text{eff}}}{\sqrt{2\pi}}\frac{\left[\ln\left(\frac{\Phi_0}{\Phi}\right)\right]^{1/2}}{\Phi}\mathrm{d}\Phi \tag{12}$$

# 2 MEM analysis of multimodal Correlation data

Based on a maximum entropy deconvolution of the ACF superposition of individual contributing species of differing diffusion times $\tau_{D,i}(R_i)$ one can write the total observable correlation function[3]

$$G(\tau) - 1 = \frac{1}{\langle N_{\text{tot}} \rangle} \sum_{\tau_{D,\min}}^{\tau_{D,\max}} \rho_i(\tau_{D,i})\, g_i(\tau, \tau_{D,i}), \tag{13}$$

$$\rho_i(\tau_{D,i}) = \Phi(R_i)^2\, c(\tau_{D,i}) \Big/ \sum_i \left[\Phi(R_i)^2\, n(\tau_{D,i})\right], \tag{14}$$

where $\rho_i(\tau_{D,i})$ are the weights of each individual correlation function $g_i(\tau, \tau_{D,i})$ belonging to a species of radius $R_i$ and corresponding diffusion time $\tau_{D,i}$ which is present in the solution with concentration $n(\tau_{D,i})$. The correct correlation functions $g_i(\tau, \tau_{D,i})$ to be used in PhoCS have been derived in[1]. However, the diffusion ensembles analyzed in this fashion for FCS data were multimodal and separated in their diffusion times by about an order of magnitude. Deconvolution of the narrow distribution of two particle sizes separated only by a factor of order unity, is however expected to be less trivial by using this method since the distributions of diffusion times $\tau_D \propto R$ will be overlapping and be difficult to tell apart. Further, the weighting depends strongly on the radius as $\Phi(R) \propto R^3$ in case of PhoCS such that the larger particles can dominate the ACFs more than in FCS. In FCS, for dye-labeled molecules or structures the signal of the diffusing species must not necessarily increase with the volume, while dyed polystyrene particles would show the same behavior. Indeed, the correlation data (see main article) visually appeared to display the slow component only, and a deconvolution by the MEM method of the two diffusing species was not possible. The ratio of the diffusion times ($\tau_D(20\,\text{nm})/\tau_{\text{D}}(30\,\text{nm})$) is on the order of unity, since both species are illuminated with the same laser intensity resulting in a higher surface temperature for the larger particles ($\propto R^3$) and thus to a speed up of diffusion that compensates the slow down of the diffusion ($\propto 1/R$) for constant temperature.

# 3 Particle size dependent detection volume

Calculations in the generalized Lorentz-Mie framework (GLMT) clearly reveal the shift from a symmetric configuration for a perfect match of heating and detection laser for small particle radii ($R < 30\,\text{nm}$) to a predominantly single lobed positive configuration for large particle radii ($R > 45\,\text{nm}$). The top right graph in figure 4 shows axial scans through the photothermal signal for varying particle radii compiled into a 2D plot. The single scans are all normalized to the maximum positive signal ($\Phi_{\max}$) for comparison reasons. The top right graph gives lateral scans at the position of maximum positive signal ($z(\Phi_{\max})$), again normalized to $\Phi_{\max}$. By fitting the individual scans with the formula for the photothermal signal (eqn 1) the detection volume parameters are extracted as depicted in the bottom graphs of figure 4. As noted for the experimental data the asymmetry parameter $z_0$ grows with increasing particle radius. Further, the axial and lateral detection volume dimension ($\omega_z$ and $\omega_\rho$) are decrease on the order of 10%.

# References

[1] M. Selmke, R. Schachoff, M. Braun and F. Cichos, *RSC Adv.*, 2012, DOI:10.1039/C2RA22061J.

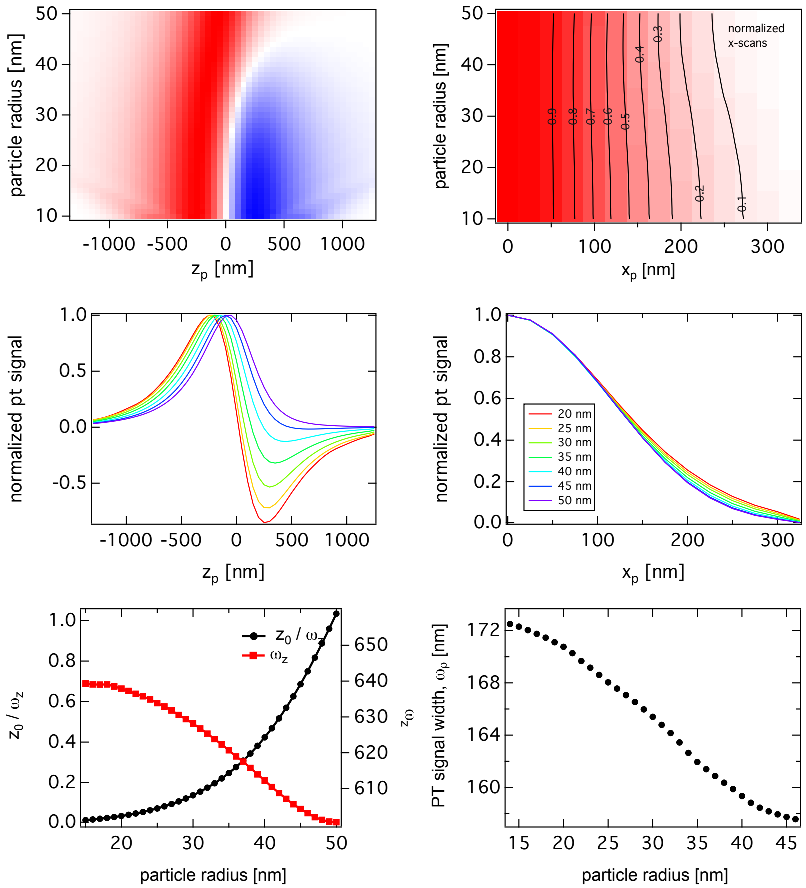


Figure 4: (top) Calculated photohtermal signal for varying particle radius in (left) axial and (right) lateral direction. (middle) line scans through the top graphs for particle radii between 20 and 50 nm in increments of 5 nm. (bottom) detection volume parameters (left) $z_0$, $\omega_z$ and (right) $\omega_\rho$ extracted from fitting the top graph's data.

[2] M. Selmke, M. Braun and F. Cichos, *ACS Nano*, 2012, **6**, 2741–2749.

[3] K. Modos, R. Galantai, I. Bardos-Nagy, M. Wachsmuth, K. Toth, J. Fidy and J. Langowski, *Eur. Biophys. J.*, 2004, **33**, 59–67.